ACS central science

Research Article

Cite This: ACS Cent. Sci. 2019, 5, 539−548

http://pubs.acs.org/journal/acscii

Cathepsin G Activity as a New Marker for Detecting Airway Inflammation by Microscopy and Flow Cytometry

Matteo Guerra,[†,‡,∥] Dario Frey,[§,∥] Matthias Hagner,[§,∥] Susanne Dittrich,[§,∥] Michelle Paulsen,[§,∥] Marcus A. Mall,[*,§,∥,⊥,#] and Carsten Schultz[*,†,∥,▽]

[†]Molecular Medicine Partnership Unit (MMPU), European Molecular Biology Laboratory (EMBL) and University of Heidelberg, 69117 Heidelberg, Germany

[‡]Faculty of Biosciences, Collaboration for Joint Ph.D. Degree between EMBL and Heidelberg University, 69117 Heidelberg, Germany

[§]Department of Translational Pulmonology, University of Heidelberg, 69120 Heidelberg, Germany

[∥]Translational Lung Research Center Heidelberg (TLRC), German Center for Lung Research (DZL), 69120 Heidelberg, Germany

[⊥]Department of Pediatric Pulmonology, Immunology and Intensive Care Medicine, Charité—Universitätsmedizin Berlin, 10117 Berlin, Germany

[#]Berlin Institute of Health (BIH), 10178 Berlin, Germany

[▽]Department of Physiology and Pharmacology, Oregon Health & Science University, 3181 SW Sam Jackson Park Road, Portland, Oregon 97239-3098, United States

Supporting Information

ABSTRACT: Muco-obstructive lung diseases feature extensive bronchiectasis due to the uncontrolled release of neutrophil serine proteases into the airways. To assess if cathepsin G (CG) is a novel key player in chronic lung inflammation, we developed membrane-bound (mSAM) and soluble (sSAM) FRET reporters. The probes quantitatively revealed elevated CG activity in samples from 46 patients. For future basic science and personalized clinical applications, we developed a rapid, highly informative, and easily translatable small-molecule FRET flow cytometry assay for monitoring protease activity including cathepsin G. We demonstrated that mSAM distinguished healthy from patient cells by FRET-based flow cytometry with excellent correlation to confocal microscopy data.

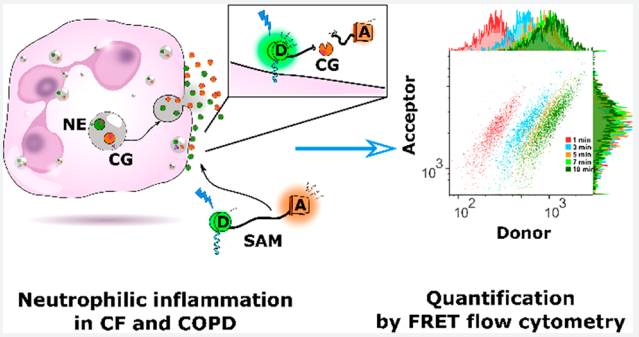

INTRODUCTION

Chronic obstructive pulmonary diseases (COPD) is the third leading cause of death in the world and encompasses a class of pathologies characterized by long-term poor airflow to the lungs.[1] Within the COPD disease family, cystic fibrosis (CF) is an autosomal recessive disorder caused by mutations in the cystic fibrosis transmembrane conductance regulator (CFTR) gene. CF is the most common lethal genetic disease in the Caucasian population. Hallmarks of both conditions are airways mucus obstruction and irreversible chronic inflammation, which elicit a massive infiltration of neutrophils into the airway lumen.[2−4] Lumen entry is promoted by neutrophil serine proteases (NSPs) such as cathepsin G (CG), neutrophil elastase (NE), and proteinase 3 (PR3), versatile enzymes secreted in the extracellular environment. Beyond penetration of the extracellular matrix, released NSPs kill pathogens and tune inflammation by cleaving cytokines of the interleukin family.[5−7] Once arrived in the airway lumen, released NSPs are usually counteracted by endogenous antiproteases (α1-protease inhibitor, α1-antichymotrypsin, α2-macroglobulin, etc.). However, on the surface of the secreting neutrophil, NSPs appear to stay inaccessible to antiproteases and are able to provoke major damage to the connective tissue.[8,9] As a result, more proinflammatory stimuli (i.e., IL-8 and IL-1) are released, engaging even more neutrophils to the site. The outcome is an irrepressible vicious circle leading to excessive and nonresolving airway neutrophilia.[9,10]

To investigate NSP activity on cell surfaces, we previously developed a ratiometric FRET reporter for neutrophil elastase (NE) to allow for the selective quantification of surface-associated NE activity. The easy readout and microscopy applicability have prompted first clinical studies which supported the relevance of NE in CF and demonstrated that membrane-bound NE activity negatively correlated with pulmonary function.[5,11−13] However, specific targeting of NE

Received: December 13, 2018
Published: February 19, 2019

DOI: 10.1021/acscentsci.8b00933
ACS Cent. Sci. 2019, 5, 539−548

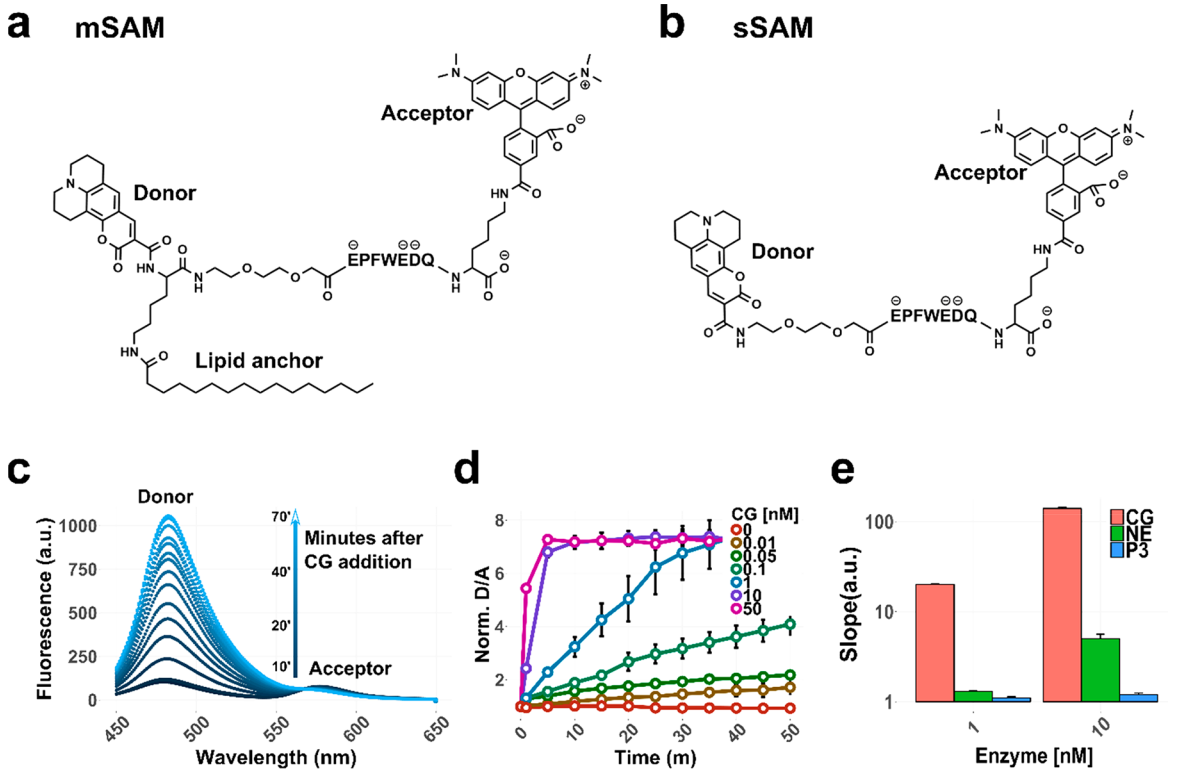

Figure 1. Chemical structures of mSAM and sSAM and their biochemical characterization. (a, b) Chemical structures. (c) Time-dependent change in fluorescence spectra of mSAM after addition of 1 nM cathepsin G (CG) measured in a phosphatidylcholine/phosphatidylserine (PC/PS) (9:1) liposome system. (d) Cleavage rates of mSAM as normalized donor/acceptor emission intensities at six different CG concentrations over time. Data are shown as mean ± SEM. (e) Linear regression slopes of mSAM cleavage rates for cathepsin G (CG), neutrophil elastase (NE), and proteinase 3 (PR3) at different enzyme concentrations. Data are shown as $\log_{10}$ of the linear regression slopes. Experiments were performed in technical triplicates.

by therapeutic inhibitors has not led to the desired results, namely, the alleviation of tissue damage.[2] This may be related to the poor accessibility of the surface-bound NE and the contribution of the other NSPs.[2,14] In addition to NE, neutrophils secrete cathepsin G, a chymotrypsin-like family member enzyme. So far, the function and interplay of this protease in CF and COPD are obscure, especially regarding its plasma membrane-associated activity, despite its involvement in the pathogenesis of various diseases,[9,13] metastatic processes,[15] its bactericidal activity,[16] and its ability to finely modulate inflammation by processing specifically cytokines like IL-36α and IL-36-β.[7,17] Hence, it is necessary to develop additional reporters as well as diagnostic tools to examine patient sputum samples. Such tools will also be useful to assess the quality of CG as new biomarker and drug target. Because of the spatial restriction of measuring protease activity by small-molecule-based FRET reporters on cell surfaces, so far, confocal microscopy was the method of choice.[11,12] However, this technique provides numerous limitations. In particular, imaging of the patient specimen is tedious, time-consuming, expensive, and limited in terms of possible functional analysis. Also, diagnostic laboratories and clinics have limited access to such highly specialized equipment. Therefore, we were interested in additional techniques suitable for higher-throughput analysis in a hospital environment. Flow cytometry provides these features and might therefore help to measure larger numbers of patient samples for a more complete understanding of protease pathophysiology. Importantly, diagnostically usable reporters applied *ex vivo* would make it possible to rapidly evaluate the response to anti-inflammatory therapies in a precise and personalized manner.

RESULTS

Here, we present the synthesis of a new pair of FRET reporters that allows the monitoring of cathepsin G activity (Figure S1). sSAM is geared toward measuring activity in human fluids (bronchial lavage, blood, and sputum supernatant), while mSAM is a lipidated cathepsin G reporter that binds to the outer leaflet of plasma membranes and monitors protease activity at the cell surface (Figure 1a,b).

We employed solid-phase peptide synthesis (SPPS) for both reporters. They feature a central peptide core EPFWEDQK flanked by a pair of fluorophores known to perform FRET in peptide-based reporters, namely, coumarin 343 as the FRET donor and TAMRA as the acceptor (Figure 1a,b and Figure S1). A dioxaoctane spacer located between the donor and the amino acid sequence helps the CG binding pocket to adapt to the recognized sequence, and increases reporter solubility and membrane impermeability.[11] mSAM also bears a palmitic acid moiety that localizes the reporter to membranes. The three negatively charged amino acids in the substrate sequence and the lipid anchor are favorable for preventing premature internalization of the reporter[18] (Figure 1a,b and Figure S1).

Precise biophysical characterization of the probes *in vitro* and in model cells demonstrated the performance level of the new cathepsin G reporters with relevance to basic and diagnostics applications. In their intact states, following donor excitation, the fluorescence emission of both probes

DOI: 10.1021/acscentsci.8b00933
ACS Cent. Sci. 2019, 5, 539−548

indicated strong quenching of the donor fluorescence due to energy transfer (Figure 1c). *In vitro* addition of human CG cleaved the peptide between Trp and Phe (Figure S2 and ref 13) and led to an 8.9-fold increase of the donor emission and a 0.9-fold decrease in acceptor fluorescence. As a result, coumarin 343 and TAMRA separated irreversibly. The ratio of donor to acceptor emission intensities over time provided a quantitative readout of reporter cleavage, which in turn was an indicator of cathepsin G activity (Figure 1c). We investigated the sensitivity of the SAM reporters by calculating cleavage rates at different CG concentrations (Figure 1d and Figure S3). The biochemical characterization of mSAM was conducted in a buffer solution containing extruded liposomes (PC/PS mixture) to simulate a membrane system. The lipidated probe showed a dynamic range ≈7−9 (donor/acceptor ratio), and mSAM was able to detect CG activity in the low picomolar range of the enzyme (Figure 1d).

A crucial feature of a successful FRET reporter is its substrate specificity. We challenged SAM reporters *in vitro* by incubating the reporter with NE and PR3, the other two main NSPs released from neutrophils (Figure 1e and Figure S3). We also investigated another member of the cathepsin family, cathepsin S (CS), and an elastase expressed by macrophages, matrix metalloprotease 12 (MMP-12) (Figure S4). None of the proteases showed any ability to cleave mSAM. Subsequently, we incubated cultured neutrophil-like cells (HL-60), which do not secrete NSPs, with active CG, NE, or PR3, respectively, at the same molar concentration. While a 3- to 4-fold ratio change was observed on CG-incubated HL-60 cells, no increase was detectable when cells were treated with NE or PR3 (Figure S5). To probe mSAM sensitivity, we incubated HL-60 cells with six different concentrations of CG and detected enzymatic activity by confocal microscopy at a CG concentration as low as 2 nM (≈2-fold increase in the D/A ratio compared to the control) (Figure S5). For a measure of cathepsin G activity with good spatial resolution, the membrane localization of mSAM needs to be stable prior to the successful cleavage event. We therefore quantified the colocalization between mSAM and the CellMask deep red plasma membrane stain and calculated a Pearson correlation coefficient of 0.58 ± 0.1 and an area overlap of 0.87 ± 0.05 between the two fluorescence channels for 101 HL-60 cells incubated with both of the molecules for 20 min (Figure S6). We also observed membrane localization in another cell line (HEK293) by imaging for 30−60 min after reporter addition (Figure S6). Even though the plasma membrane retention was no longer than this time-span (also roughly the retaining time for the membrane stain), it was sufficient to monitor activity on patient neutrophils in which the cleavage is very fast and rapidly detectable because of the high sensitivity of the reporter. mSAM permitted confocal microscopy of human neutrophils, and the calculated D/A ratio provided a measure of membrane-bound CG activity (Figure 2a). Cells were isolated from sputum by incubation with concentrated dithiothreitol and subsequent washing to separate soluble fractions of proteases. Neutrophils are easily identified by their segmented nuclei (Figure 2a, DNA stain, orange arrowheads). To directly show that surface-bound CG is highly activated in chronic airway inflammation, we analyzed the sputum of 24 subjects (10 healthy and 14 CF) by microscopy. While we detected a neglectable enzymatic activity in the control group (1.16-fold ±0.35), CF neutrophils showed a 3.03 ± 1.51 donor/acceptor increase in CG activity ranging from 1.4 to 4.9

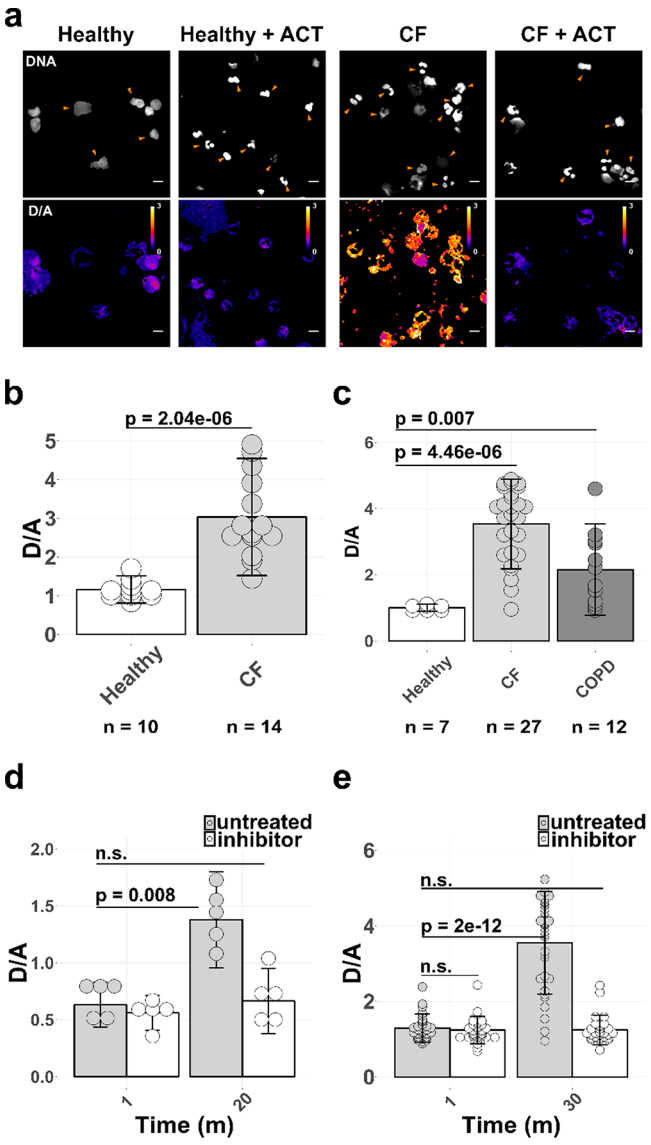

Figure 2. Airway inflammation features increased CG activity. (a) Representative confocal images of sputum-derived human neutrophils (DNA panel, orange arrowheads) incubated with mSAM (D/A panel). (b) Quantification of cathepsin G (CG) activity on 14 CF and 10 healthy donor neutrophils by confocal microscopy (mSAM). (c) Donor/acceptor increase after 30 min of incubation of sSAM with sputum supernatants (7 healthy donors and 27 CF patients) and 12 COPD bronchial lavage (BL) fluids. (d) Mean donor/acceptor values of 5 patients after 1 and 20 min of incubation with mSAM in the presence or absence of ACT [3 μM]. (e) Fluorimetric quantification of CG activity in the mucus supernatants of CF patients in the presence of a small-molecule CG inhibitor I (CGI) [25 μM], 1 and 30 min after sSAM addition. Scale bars: 10 μm. Images are representative of the 14 and 10 subjects shown in part b. For each condition and patient, 50−100 cells were analyzed by microscopy. Each human sample was measured in duplicate. Statistics were calculated by Wilcoxon rank sum test.

(Figure 2b, Figure S7 and Table S1). We also employed sSAM to monitor CG activity present in 27 CF patient sputum supernatants and 12 COPD bronchial lavage (BL) fluids: the incubation of the samples with sSAM for 30 min resulted in a 3.53 ± 1.35 donor/acceptor change in CF and 2.15 ± 1.38 in COPD compared to the 1 ± 0.10 observed in 7 healthy subjects (Figure 2c, Figure S8 and Tables S2 and S3).

DOI: 10.1021/acscentsci.8b00933
ACS Cent. Sci. 2019, 5, 539−548

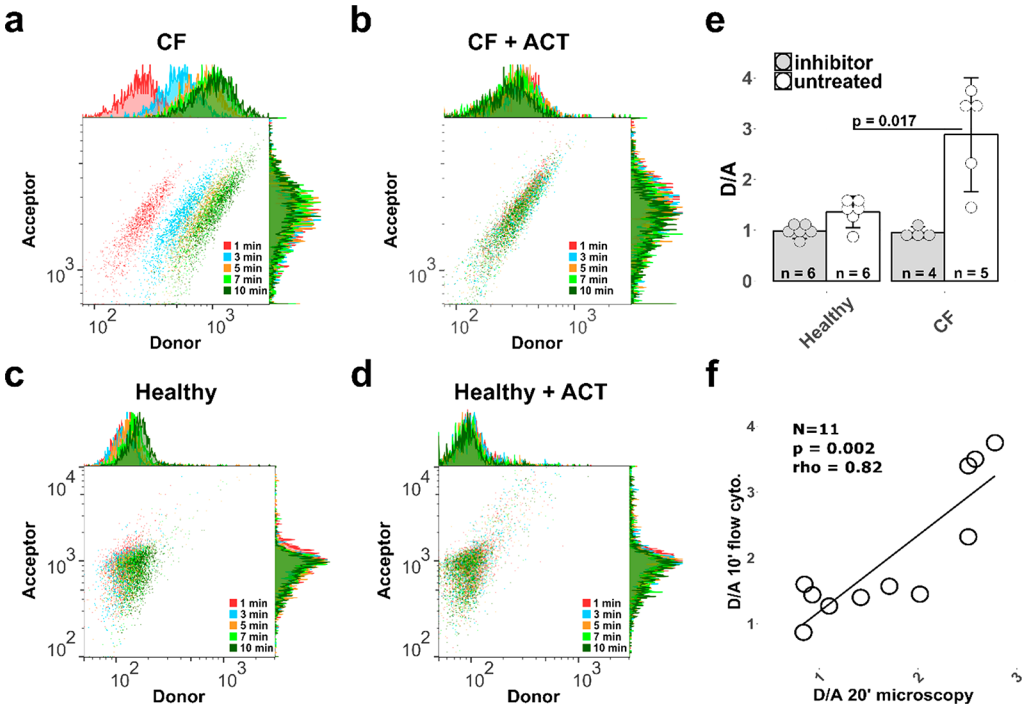

Figure 3. Introducing small-molecule FRET flow cytometry. (a–d) Representative flow cytometry neutrophil-specific ratiometric measurement of surface-bound CG activity at different time points after mSAM addition. (e) Average D/A ratio measured on sputum neutrophils derived from 11 human subjects (6 healthy donors and 5 CF) after 10 min and (f) their correlation with the respective microscopy measurement (n = 50–70 for microscopy, $n \geq 1000$ for flow cytometry). Data are represented as mean ± SD. Each human sample was measured in duplicate. Statistics were calculated by Wilcoxon rank sum and Spearman rank correlation tests.

Finally, we tested SAM reporter specificity directly on patient specimens (Figure 2d,e and Figure S9). By incubating the main endogenous CG antiprotease (α1-antichymotrypsin, ACT) with cells derived from five CF patients, we were able to abolish almost any detectable enzymatic activity (Figure 2d, and Figure S9). We then incubated sputum cells from three CF patients with Cathepsin G Inhibitor I (CGI; CAS 429676-93-7) which abolished any increase in the signal, and with two different concentrations of Sivilestat (CAS 127373-66-4), a selective NE inhibitor, resulting in no differences between untreated and Sivilestat-treated cells (Figure S9). This further demonstrates that our reporter is not significantly cleaved by membrane-bound neutrophil elastase. In the same fashion, the CGI suppressed any donor/acceptor increase in CF sputum supernatants when sSAM was present (Figure 2e).

Another protease which, if present, may interfere with our assay is human chymase: a chymotrypsin- and cathepsin-G-like protease found in secretory granules of mast cells.[19] Chymase has been linked to the development and propagation of allergic inflammation in asthma.[20,21] Since the role of this enzyme in CF and COPD has been poorly investigated, and given that CGI inhibits cathepsin G and chymase equally, we tested the patient samples for their chymase content. First, we checked the specificity of our reporter: chymase cleaved sSAM more rapidly than any other protease we tested except cathepsin G (Figures S3 and S10). The latter was able to hydrolyze the reporter 2.5 to 8 times faster when the two enzymes were incubated at the same molar concentration (Figure S10). In addition, we quantified chymase activity by a commercial chymase activity assay kit (CS1140) in 10 CF sputum samples and 6 COPD lavages (Figure S10) employing the *N*-succinyl-Ala-Ala-Pro-Phe p-nitroanilide substrate. We demonstrated that this substrate is cleaved 23–89 times slower by cathepsin G than chymase (Figure S10 and refs 22–24). The resulting active chymase concentration (undetectable in COPD and 24.7 ± 14.4 nM in CF) cannot account for the high signal observed upon incubation of sSAM with the same CF samples (Figure S10) and the ones measured in Figure S8. Finally, we quantified the overall chymase concentration in 16 CF and 7 COPD samples via an ELISA (human mast cell chymase ELISA kit, EKC34542). We detected an average of 6.5 ± 4.03 and 0.1 ± 0.1 nM chymase, respectively (Figure S10). At 6.5 nM concentration, chymase can only generate 1.4% of the cathepsin G signal in Figure S10 and even less of the data reported in Figure S8.

Taken together, this proves that, within the dense protease mixture present in patient sputum, we could selectively monitor cathepsin G and fully address its relevance in airway inflammation (Figure 2d,e and Figures S9 and S10).

As shown, microscopy of patient neutrophils is a powerful technique for studying spatially confined protease activity. However, it is limited by the availability of high-end microscopes, extensive data acquisition, and image analysis procedures. Moreover, human mucus is a variable and complex biological matrix that contains debris and dying cells which are almost impossible to exclude. Finally, the massive neutrophilic infiltration in inflamed lungs makes microscopy unpractical for the study of rare cell populations, such as macrophages, whose MMP-12 role in CF has not been fully elucidated yet, even though the enzyme plays a crucial role in the pathogenesis of asthma and COPD.[25]

To overcome these limitations and to complement microscopy with an alternative technique, we applied mSAM in flow cytometry. We combined flow cytometry—which allows us to gate any cell population present in the sputum[26]—with the ability of mSAM to bind to the cell surface where it

DOI: 10.1021/acscentsci.8b00933
ACS Cent. Sci. 2019, 5, 539–548

functions in the same way as any other marker or antibody routinely used in flow cytometry, with the difference that the intrinsic nature of mSAM as a small-molecule FRET reporter was exploited to quantify a specific enzymatic activity. Cells were isolated from mucus in the same way as for the microscopy experiment, and neutrophils were selectively gated (Figure S11). A cathepsin-G-dependent increase in the donor/acceptor coming from patient neutrophils incubated with mSAM was observed over time (Figure 3a). Incubation of patient cells with ACT abolished the effect (Figure 3b). As expected, no response was observed from healthy-subject-derived cells (Figure 3c,d). To determine if data obtained by small-molecule FRET flow cytometry recapitulate the results of microscopy, we performed paired analysis and quantified the average D/A ratio for 11 subjects (5 CF and 6 healthy) (Figure 3e) obtaining a significant correlation (ρ = 0.82; p = 0.002) between flow cytometry and confocal microscopy (Figure 3f).

DISCUSSION

For the successful mobilization of primary granules, neutrophils need to be primed with chemoattractants and then challenged with activating and/or proinflammatory stimuli. In cystic fibrosis airways, this process is mediated by the action of TNFα and IL-8 and potentially other activating factors that are contained in the chronically inflamed and infected microenvironment of CF airways. All together, these stimuli are potent inducers of NSPs secretion.[27] In previous studies, we and others found that neutrophil elastase (NE) is elevated at the surface of CF airway neutrophils.[5,12,28] Similarly, we found that macrophage elastase (MMP12) is elevated on macrophages sampled from CF airways.[29] These data are consistent with the concept that neutrophils (and macrophages) are chronically activated in the unique microenvironment of CF and COPD airways and that this activation leads to increased secretion of proteases and their binding on the cell surface. Our findings add cathepsin G as an additional actor in inflamed CF and COPD airways, possibly involved in the pathogenesis of these conditions and representing a potential drug target. A scenario where the orchestrated action of different NSPs contributes to lung disruption is therefore emerging and needs to be considered for predicting COPD symptoms in risk populations as well as for successful drug testing in clinical trials and for monitoring the effect of drug treatment in individual patients.

With the NEmo and SAM series of reporters, we now have the tools to monitor, in a spatially resolved fashion, the activity of the two major neutrophil proteases (representing the chymotrypsin- and trypsin-like families). The probes show a very similar dynamic range (7−9.5 for both). sSAM has a slightly higher limit of detection than the corresponding soluble NEmo-1 (2−3 versus 0.3 nM) while the lipidated reporters (mSAM and NEmo-2) display almost identical sensitivity and limit of detection. NEmo-2 resides longer at the plasma membrane (1−2 h) compared to mSAM (0.5−1 h); in both cases this is sufficient for microscopy and flow cytometry applications where only 10−20 min is required to complete the assay.

The employment of small-molecule FRET flow cytometry showed outstanding results in terms of sensitivity, throughput, and reproducibility of the microscopy results. Notably, the time necessary to measure and analyze more than 1000 patient neutrophils is reduced to roughly 30 min compared to the several hours that microscopy needs for analyzing 50−100 cells. Our advanced multicolor flow cytometry setup, in combination with the capabilities of our reporters, allows the selective gating of almost any cell population and subpopulation present in patient sputum or derived from many different biological samples. At the same time, it quantifies a spatially localized enzymatic activity in a ratiometric fashion.

This novel technology will foster a better understanding of protease pathophysiology not only in CF and COPD but also whenever protease-driven inflammation comes into the game. We envision that the introduction of SAM and other available small-molecule[30] or semisynthetic energy-transfer-based reporters[31,32] into the flow cytometry technology will speed up basic and clinical research and facilitate the translation of the results into the clinical arena. Importantly, this technique will help monitoring disease progress in high-risk COPD candidates and anti-inflammatory drug effectiveness at an individual level with very low invasiveness and in an economically tolerable fashion.

MATERIALS AND METHODS

Chemicals and Reagents. Standard solvents for peptide chemistry were from Fluka, Sigma-Aldrich (Steinheim, Germany), and Novabiochem (Darmstadt, Germany). COMU 1-[(1-(cyano-2-ethoxy-2-oxoethylideneaminooxy) dimethylaminomorpholino)] uronium hexafluorophosphate was from Merck KGaA (Darmstadt, Germany); Fmoc−lys(Mtt) Wang resin and Fmoc-amino acids were from Novabiochem. [2-[2-(Fmocamino)ethoxy]ethoxy]acetic acid (Fmoc-OcO_2-OH; PEG-linker) was from Iris Biotech (Marktredwitz, Germany). Coumarin 343 carboxylic acid was from Merck KGaA (Darmstadt, Germany). 5(6)-TAMRA NHS ester was purchased from AnaSpec.

Enzymes and Inhibitors. Human neutrophil elastase and proteinase 3 were from Merck KGaA (Darmstadt, Germany) and cathepsin G was from Elastin Products Company Inc. (Owensville, MO). α1-Antichymotrypsin from human plasma and cathepsin G inhibitor I were from Merck KGaA (Darmstadt, Germany). Recombinant cathepsin S and MMP12 were from R&D Systems (Minneapolis, MN). Human chymase (BML-SE281-0010) was from Enzo Life Sciences, Inc. (Farmingdale, NY). The chymase activity assay kit (CS1140) was from Merck KGaA (Darmstadt, Germany). Human mast cell chymase ELISA (EKC34542) was from Biomatik. Sivilestat (S7198) was from Merck KGaA (Darmstadt, Germany).

Synthesis of the Reporters. sSAM and mSAM were synthesized by standard Fmoc-solid-phase peptide synthesis starting from a Wang resin loaded with Fmoc−lysine(Mtt)−OH. Fmoc deprotection was achieved by treating with 20% piperidine/DMF (v/v) for 5 min (three times) and following the completion of the reaction by monitoring loss of Fmoc absorption. Amino acids (3 equiv) are coupled by *in situ* activation with COMU/DIPEA (3:4 equiv) for 45 min (two times). Capping of unreacted amino groups is obtained by treatment with acetic acid (96%)/pyridine (1:9) two times for 5 min. Every coupling, deprotection, and capping step was followed by 3−5 washing cycles with DMF. Fluorophores (3 equiv of coumarin 343 carboxylic acid, 2 equiv of 5(6)-TAMRA NHS ester) were coupled by *in situ* activation with COMU/DIPEA (3:4 equiv) for coumarin and 6 equiv of DIPEA for TAMRA, with shaking for 45 min and repeating two times. For sSAM, the methyltrityl group of the C-terminal lysine was deprotected (TFA/TIS/DCM 1:2:97, 4 min, seven

DOI: 10.1021/acscentsci.8b00933
ACS Cent. Sci. 2019, 5, 539−548

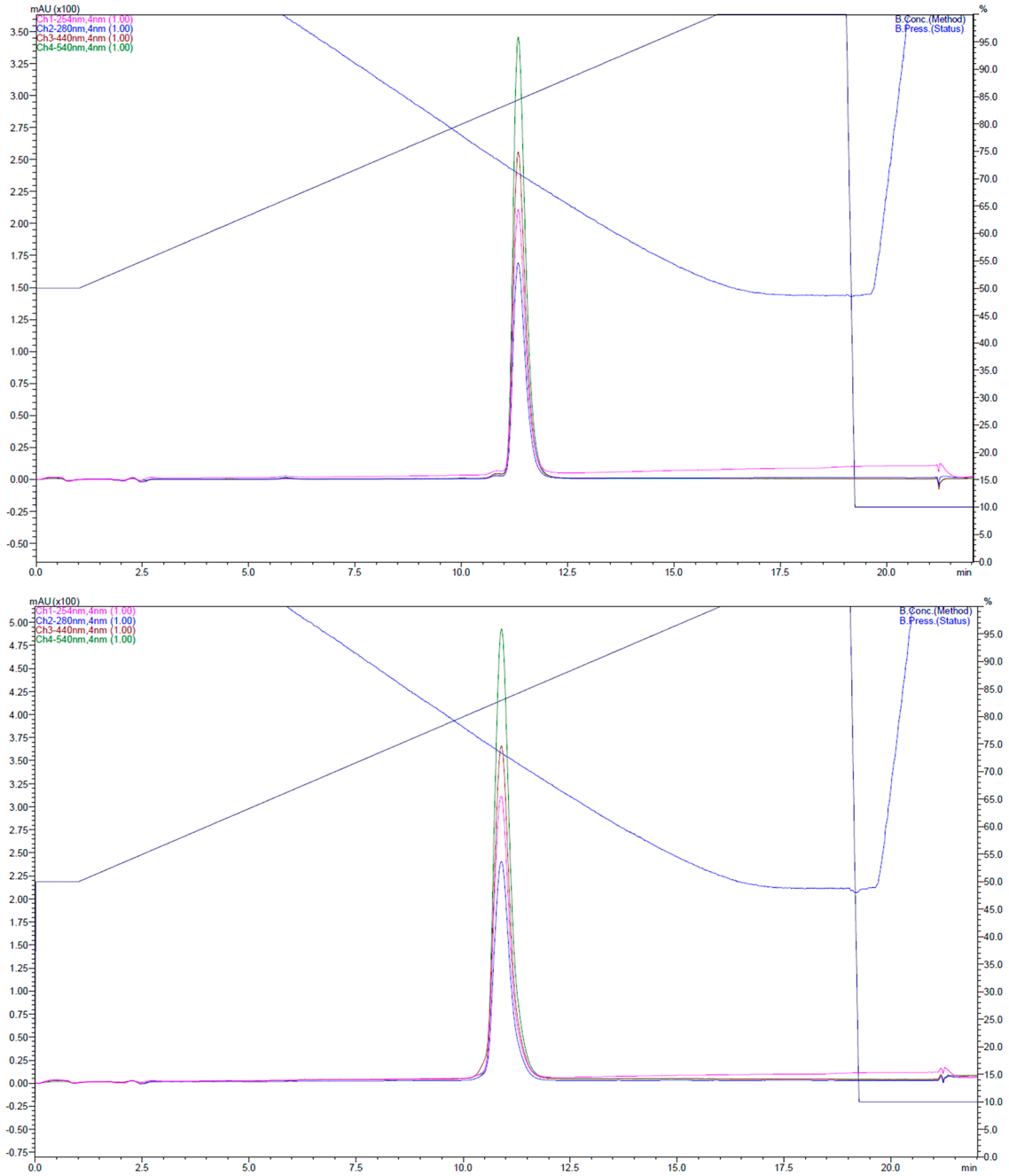

Figure 4. Analytical HPLC of purified mSAM. Gradient of 50−100% acetonitrile. RT: 10.7 min (lower panel), 11.5 min (upper panel). Absorbances at 450 nm (coumarin 343), 540 nm (TAMRA), 254 nm, and 280 nm are shown. Both 5-(6-)TAMRA isomers are shown separately (upper and lower panel).

times), and TAMRA was coupled. Finally, the N-terminal Fmoc group was deprotected, and coumarin 343 was coupled. For mSAM, the coupling of TAMRA to the C-terminal lysine was performed first. Then, the N-terminal lysine (palmitic acid) was Fmoc-deprotected and coumarin-343-coupled. The reporters were cleaved off the resin by shaking with TFA/TIS/water (96:2:2) for 2 h, and then washed with diethyl ether for concentration under vacuum, dissolved in 50% acetonitrile/water (v/v), and analyzed by HPLC.

Reporter Purification. sSAM and mSAM were analyzed and purified by RP-HPLC on a Shimadzu system equipped with a photodiode array detector (Duisburg, Germany). Analytical runs were performed on an RP-18 column (NUCLEODUR C18 ec 5 μm, 4 mm × 250 mm, Macherey-Nagel, Düren, Germany) using a linear gradient from 10% to 100% or from 50% to 100% acetonitrile with 0.05% trifluoroacetic acid and a flow rate of 1.5 mL/min (Figures 4 and 6). Purification was performed by preparative RP-HPLC using a Discovery Bio Wide Pore C18 column (NUCLEODUR 100-5 C18 ec, 10 mm i.d. × 250 mm, Macherey-Nagel, Düren, Germany), detecting at 254, 280, 440, and 540 nm and using a gradient of 50−100% (mSAM) or 10−100% (sSAM) acetonitrile with 0.05% trifluoroacetic for 30 min and a flow rate of 5 mL/min. sSAM and mSAM were analyzed ions by mass spectrometry as multiple charged (Figures 5 and 7).

DOI: 10.1021/acscentsci.8b00933
ACS Cent. Sci. 2019, 5, 539−548

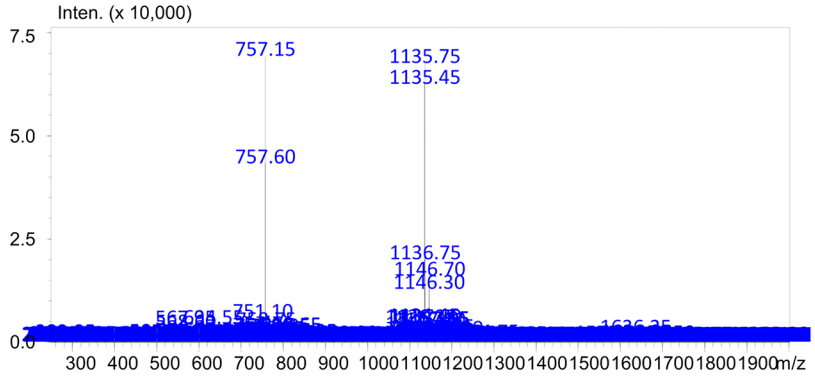

Figure 5. Mass spectra mSAM. Expected masses: $[M+1]^{+}$, 2269.10; $[M+2]^{2+}$, 1134.5; $[M+3]^{3+}$, 756.7.

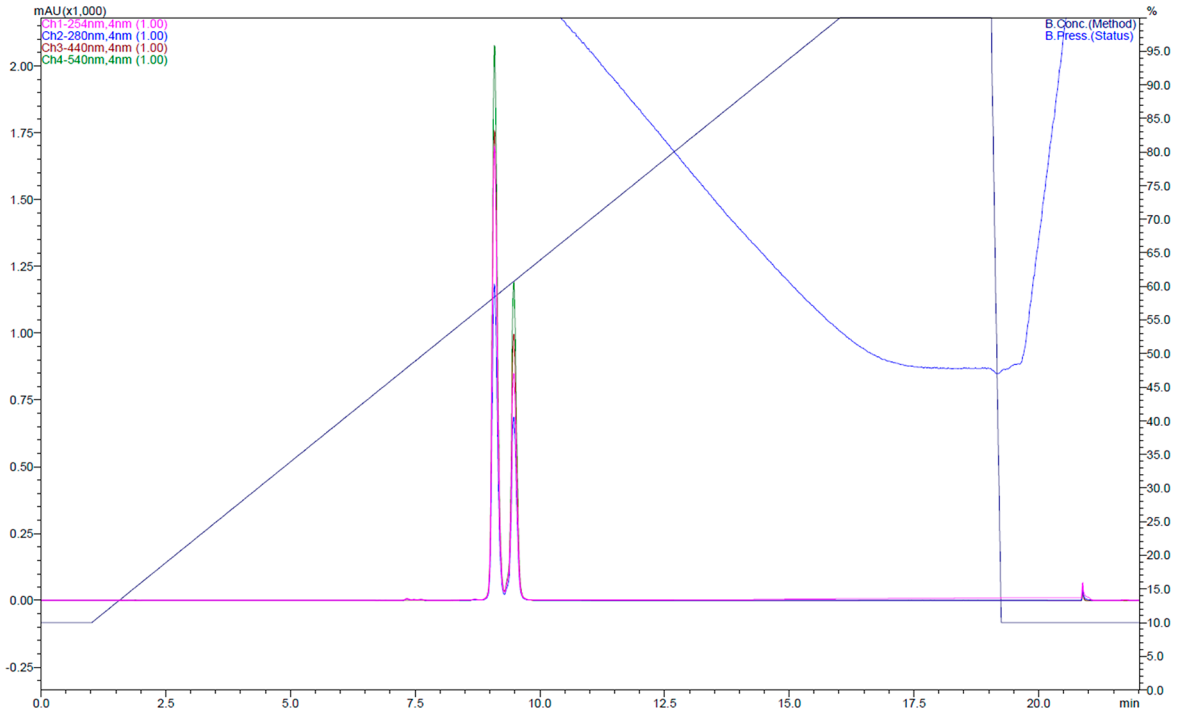

Figure 6. Analytical HPLC of purified sSAM. Gradient of 10−100% acetonitrile, RT: 9 and 9.5 min. Absorbance at 450 nm (coumarin 343), 540 nm (TAMRA), 254 nm, and 280 nm are shown. The two peaks represent the two 5-(6-)TAMRA isomers.

***In Vitro* Measurements.** NE, PR3, CG, and CS activities were measured in 100 mM TrisHCl pH 7.5, 500 mM NaCl. MMP12 was measured in 50 mM TrisHCl pH 7.5, 10 mM $CaCl_2$, 150 mM NaCl, 0.05% (w/v) Brij-35. mSAM assays were conducted in a 1 mM liposome solution prepared of phosphatidylcholine/phosphatidylserine (PC/PS) (9:1) (Avanti Polar Lipids, Inc., Alabaster, AL) according to the manufacturer's protocol. mSAM assays were performed with a JASCO spectrofluorometer (FP-8500, JASCO Deutschland GmbH) at 25 °C. sSAM assays were performed in black polystyrene 96-well half area assay plates with a fluorescence plate reader (Enspire 2300, PerkinElmer, Waltham, MA) at 25 °C. Both reporters were used at a final concentration of 2 μM. For mSAM measurements, human enzymes were added, and reporter cleavage was followed by recording emission spectra every 5 min over a period of 20−70 min with the settings: λ_{exc} = 430 nm, λ_{em} = 450−650 nm. For sSAM measurements, human enzymes were added, and the emission maxima of donor (485 nm) and acceptor (580 nm) fluorophores after 405 nm excitation were recorded every 90 s over a period of 60 min and plotted as D/A ratio. All sSAM measurements were performed in technical duplicates. All mSAM measurements were performed in technical triplicates.

Cell Culture and *in Vivo* mSAM Characterization. HEK293 cells were passaged and maintained in DMEM (high glucose; Thermo Fisher) supplemented with 10% FBS (Biowest), 1% GlutaMAX (Thermo Fisher), 1% sodium pyruvate (Thermo Fisher), 1% NEAA (Thermo Fisher), and 1% Pen Strep (Thermo Fisher). For imaging experiments, 30 000 cells were plated on an 8-well Lab-Tek chamber slide (Merck, Darmstadt, Germany) overnight, and medium was replaced before imaging with a live cell imaging solution (Nr. A14291DJ, Thermo Fisher). mSAM was added to a final concentration of 1 μM. Cells were imaged by confocal microscopy in time series of 30−60 min recording every 2 min at 37 °C and 5% CO_2. Data were collected in three independent experiments.

HL-60 cells were passaged and maintained in RPMI 1640 (Gibco 21875-034) supplemented with 12.5% HI-FBS (GIBCO 10082) and primocin [50 mg/mL] (Invivogen).

DOI: 10.1021/acscentsci.8b00933
ACS Cent. Sci. 2019, 5, 539−548

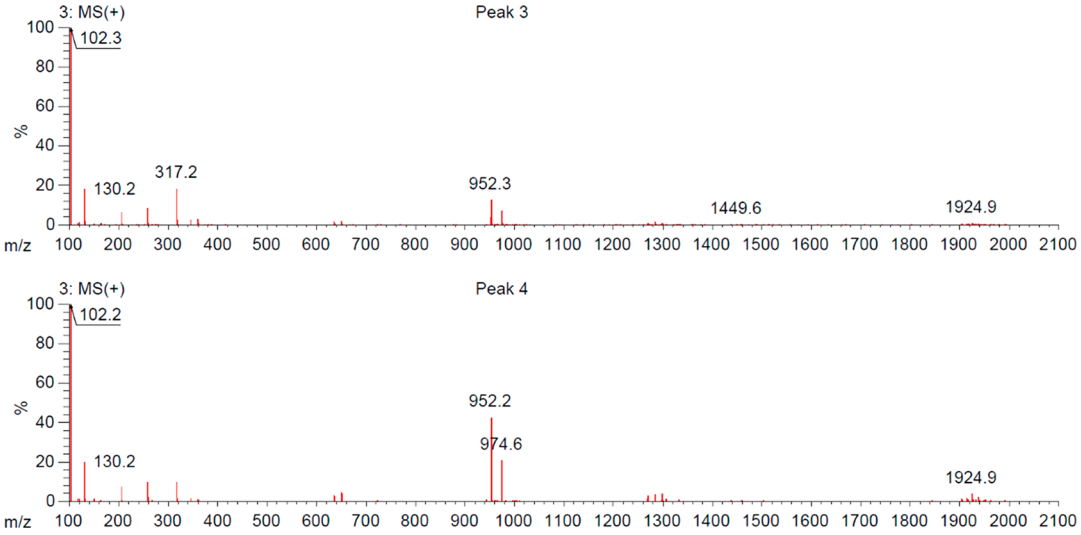

Figure 7. Mass spectra of sSAM. Expected masses: $[M+1]^+$, 1902; $[M+2]^{2+}$, 951; $[M+3]^{3+}$, 634. The two spectra correspond to the two isomer peaks observed by HPLC (Figure 6).

For colocalization experiments, 70 000 cells were incubated with mSAM [1 μM] and cell mask deep red plasma membrane stain (Thermo Fisher scientific, catalog C10046) (1:1000 dilution) for 20 min in 1.5 mL Eppendorf tubes. Then, cells were cytospun on microscopy slides, fixed for 10 min in ice cold methanol, and mounted with Roti-Histokitt (Carl Roth, Karlsruhe, Germany). For sensitivity and specificity experiments, 30 000 cells were incubated with mSAM [1 μM], Draq5 DNA stain (BioStatus Limited, Shepshed, U.K.) (1:1000 dilution) and the appropriate enzyme (NE, CG, and PR3 at final concentration of 100 nM) for 20 min in 1.5 mL Eppendorf tubes. Then, cells were cytospun on microscopy slides, fixed for 10 min in ice cold methanol, and mounted with Roti-Histokitt (Carl Roth, Karlsruhe, Germany). Data were collected in two independent experiments.

Sputum Processing and Membrane-Bound CG Activity Measurements. Sputum was separated from saliva by adding 4 volumes of 10% Sputolysin solution (Calbiochem, Darmstadt, Germany) followed by 15 min of mild shaking at room temperature. Cells were then diluted by adding the same volume of PBS and filtered through 100 and 40 μm cell strainers. For the separation of cells from the soluble fraction of proteases, cells were centrifuged at 300*g* and 4 °C for 10 min. Cell pellets were resuspended in PBS and counted.

In 50 μL of PBS, 30 000 human CF or healthy donor sputum cells were incubated with mSAM [2 μM], Draq5 DNA stain (BioStatus Limited, Shepshed, U.K.) (1:1000 dilution), for 20 min at room temperature in 1.5 mL Eppendorf tubes. As negative controls, cells were preincubated for 10−15 min at room temperature with either 3 μM of α_1-antichymotrypsin from human plasma (ACT) (Merck KGaA, Darmstadt, Germany), 5 μM of cathepsin G inhibitor I (CGI) (CAS 429676-93-7, Merck, Darmstadt, Germany), cOmplete Protease Inhibitor Cocktail with EDTA (Merck, Darmstadt, Germany), or Sivilestat (S7198, Merck, Darmstadt, Germany). For the determination of the initial noncleaved FRET ratio, mSAM was added to cells preincubated with inhibitors and moved to ice after only a 1 min incubation. For the determination of mSAM specificity, the reporter was added to cells preincubated with CGI or ACT and left for 20 min at room temperature. Finally, reactions were quenched at different time points by adding 100 μL of ice cold PBS, and cells were quickly cytospun on microscopy slides, fixed for 10 min in ice cold methanol, and mounted with Roti-Histokitt (Carl Roth, Karlsruhe, Germany). Experiments were performed in technical duplicates for each of the human subjects.

Confocal Microscopy of Human Sputum. Images were acquired using a Leica SP8 confocal microscope (Leica Microsystems, Wetzlar, Germany) equipped with an HC PL APO CS2 40×/1.3 oil objective. DRAQ5 was excited with a 633 nm HeNe laser, and emission was recorded between 650 and 715 nm. Coumarin 343 was excited with a 458 nm argon laser. Donor emission was recorded between 470 and 510 nm and acceptor emission between 570 and 610 nm. The pinhole was set to 195.9 μm (3.0 AU) for the two sequential channels. For the quantification of membrane-bound CG activity, the ratio of donor to acceptor fluorescence after 1 and 20 min of incubation with mSAM was calculated. Ratios were normalized to the values obtained from cells treated with inhibitor and incubated for 1 min with the reporter, which represents the noncleaved state of the probe. Images from technical duplicates for each of the 24 human subjects were acquired.

Soluble CG Activity Measurements. Cell-free sputum supernatant was diluted in 100 mM TrisHCl pH 7.5, 500 mM NaCl (CF diluted 1:20, healthy donors diluted 1:10, COPD BL 1:1). All kinetic assays were performed at 25 °C using a fluorescence plate reader (Enspire 2300, PerkinElmer, Waltham, MA). As negative control, sputum supernatants were preincubated with 25 μM cathepsin G inhibitor I (CAS 429676-93-7, Merck, Darmstadt, Germany) for 15 min at room temperature. For quantification of CG activity with sSAM, 40 μL of supernatant was added in polystyrene 96-well half area assay plates (Corning Inc., Acton, MA). Finally, sSAM was added to a final concentration of 2 μM, and reporter cleavage was recorded over time using the following settings: λ_{exc} = 405 nm, λ_{em} = 485 nm, and λ_{em} = 580 nm. Standard curves from known concentrations of CG were included in each assay. All measurements were performed in technical duplicates. For quantification of the concentration of active cathepsin G in CF and COPD samples, a standard curve from known concentrations (1−0.0156 μg/mL) of cathepsin G was

DOI: 10.1021/acscentsci.8b00933
ACS Cent. Sci. 2019, 5, 539−548

included. Then, concentrations were calculated via interpolation of the measured slopes (linear fitting).

Chymase Activity and ELISA Measurements. The chymase activity assay was performed according to manufacturer protocol, with CF samples diluted (1:20) in 100 mM TrisHCl pH 7.5, 500 mM NaCl. COPD BL was left undiluted. All kinetic assays were performed at 25 °C using a fluorescence plate reader (Enspire 2300, PerkinElmer, Waltham, MA). For quantification of the concentration of active chymase in samples, standard curves from known concentrations of human chymase (BML-SE281-0010) (2−0.032 μg/mL) were included in each assay. For a demonstration of the preferential cleavage of Succ-AAPF-pNA by chymase over cathepsin, different concentrations of human chymase (BML-SE281-0010) and cathepsin G (Elastin Products Company Inc.) were incubated with the same concentration of substrate according to manufacturer protocol, respectively. Chymase ELISA and quantification was performed according to manufacturer protocol. CF samples diluted were diluted 1:20. COPD BL was left undiluted.

FRET Flow Cytometry. Cells were isolated from sputum as described above, and 1×10^6 cells were resuspended in 100 μL of PBS. Prior to surface staining with specific monoclonal fluorochrome-conjugated antibodies or respective isotype control antibodies, cells were incubated with FcBlock (BD Biosciences, Heidelberg, Germany). For the detection of sputum neutrophils,[26,33] cells were stained with CD14-Pe-Cy7 (Clone M5E2) (BD Biosciences, Heidelberg, Germany), CD16-Alexa Fluor 700 (Clone 3G8) (BD Biosciences, Heidelberg, Germany), CD45-APC-Cy7 (Clone 2D1) (BD Biosciences, Heidelberg, Germany), CD66b-Pe-Dazzle 594 (Clone G10F5) (Biolegend, San Diego, CA), and CD169-Alexa Fluor 647 (Clone 7-239) (Biolegend, San Diego, CA) for 30 min at 4 °C, resuspended in 200 μL of PBS followed by a viability staining with 7AAD according to manufacturer's instructions (Biolegend, San Diego, CA). Sputum neutrophils were defined as $CD45^+CD16^+CD66b^+CD14^-CD169^-$. For the measurement of CG activity by flow cytometry on sputum neutrophils, mSAM [2 μM] was added to surface-stained cells, and subsequently flow cytometry was performed at 0, 1, 3, 5, 7, 10, 15, and 20 min on each of the 5 healthy donors and 6 CF patients analyzed. At least 1000 neutrophils were recorded for each condition. For inhibition of CG activity and specificity control of the reporter, surface-stained cells were incubated with 50 μM cathepsin G inhibitor I (CAS 429676-93-7, Merck, Darmstadt, Germany) or 20 μM α_1-antichymotrypsin from human plasma (Merck KGaA, Darmstadt, Germany) for 10 min at room temperature followed by addition of mSAM. Inhibited CG activity was measured by flow cytometry at the corresponding time points. Flow cytometry was performed on a LSRFortessa flow cytometer (BD Biosciences, Heidelberg, Germany) equipped with 3 lasers at wavelengths of 405, 488, and 633 nm. For the detection of CG activity, the probe was excited with the 405 nm laser, and the donor signal was detected between 425 and 475 nm (filter 450/50 nm) and the acceptor signal between 564 and 606 nm (filter 585/42 nm) with an upstream long-pass filter that reflected light below 550 nm. CG activity was measured on at least 1000 neutrophils at each time point. Data were analyzed with FACS Diva software v8.0.1 (BD Biosciences, Heidelberg, Germany) or Flow Jo software v10 (Treestar, Ashland, OR). FRET ratio was calculated by division of donor (450/50 nm) and acceptor (585/42 nm) channel values measured on the gated neutrophils over time and normalized to the donor/acceptor measured after 1 min addition of reporter on cells preincubated with inhibitor for 10 min.

Statistics. All statistical tests were performed using R software (R version 3.4.4) and GraphPad version 6.01. Two-tailed Wilcoxon rank sum test, Spearman's rank correlation coefficient tests, and linear or 4PL fitting to standard curves were applied when appropriate.

Data Availability. The FIJI macro FluoQ used for image analysis and quantification is available at ref 34. The scripts used for data processing and statistics as well as all the raw data are all available upon request.

Human Samples. Informed written consent was obtained from all subjects prior to sample collection. The study was approved by the appropriate ethical committee of Heidelberg University.

Significant Hazards or Risks Statement. No unexpected or unusually high safety hazards were encountered.

■ ASSOCIATED CONTENT

Supporting Information

The Supporting Information is available free of charge on the ACS Publications website at DOI: 10.1021/acscentsci.8b00933.

Reporter purification; mSAM donor fragment localization, cleavage site, sensitivity and specificity, characterization; membrane-bound CG activity single patient data; soluble CG activity single patient data; *in vivo* specificity of mSAM; human mast cell chymase activity and concentration; and flow cytometry gating strategy (PDF)

■ AUTHOR INFORMATION

Corresponding Authors

*E-mail: marcus.mall@charite.de.
*E-mail: schulcar@ohsu.edu.

ORCID

Carsten Schultz: 0000-0002-5824-2171

Author Contributions

M.G., M.A.M., and C.S. designed the experiments and wrote the manuscript. M.G. performed all the experiments and analyzed data. D.F. performed plate reader sSAM characterization and flow cytometry experiments. M.H. performed flow cytometry experiments. S.D. and M.P. provided patient samples.

Notes

The authors declare no competing financial interest.

■ ACKNOWLEDGMENTS

We are grateful to Malte Paulsen (EMBL flow cytometry core facility) for helpful discussion. We thank members of both research groups for critical discussion of the experiments. We would like to thank Matilde Bertolini for critical reading of the manuscript and support. This work was supported by German Ministry for Education and Research (82DZL00401, 82DZL004A1) and Einstein Foundation Berlin (EP-2017-393).

■ REFERENCES

(1) Wang, H.; Naghavi, M.; Allen, C.; Barber, R. M.; Bhutta, Z. A.; Carter, A.; Casey, D. C.; Charlson, F. J.; Chen, A. Z.; Coates, M. M.;

DOI: 10.1021/acscentsci.8b00933
ACS Cent. Sci. 2019, 5, 539−548

et al. Global, Regional, and National Life Expectancy, All-Cause Mortality, and Cause-Specific Mortality for 249 Causes of Death, 1980−2015: A Systematic Analysis for the Global Burden of Disease Study 2015. *Lancet* **2016**, *388* (10053), 1459−1544.
(2) Owen, C. A. Roles for Proteinases in the Pathogenesis of Chronic Obstructive Pulmonary Disease. *Int. J. Chronic Obstruct. Pulm. Dis.* **2008**, *3* (2), 253−268.
(3) Barnes, P. J.; Shapiro, S. D.; Pauwels, R. A. Chronic Obstructive Pulmonary Disease: Molecular and Cellular Mechanisms. *Eur. Respir. J.* **2003**, *22* (4), 672−688.
(4) Elborn, J. S. Cystic Fibrosis. *Lancet* **2016**, *388* (10059), 2519−2531.
(5) Gehrig, S.; Duerr, J.; Weitnauer, M.; Wagner, C. J.; Graeber, S. Y.; Schatterny, J.; Hirtz, S.; Belaaouaj, A.; Dalpke, A. H.; Schultz, C.; et al. Lack of Neutrophil Elastase Reduces Inflammation, Mucus Hypersecretion, and Emphysema, but Not Mucus Obstruction, in Mice with Cystic Fibrosislike Lung Disease. *Am. J. Respir. Crit. Care Med.* **2014**, *189* (9), 1082−1092.
(6) Pham, C. T. N. Neutrophil Serine Proteases: Specific Regulators of Inflammation. *Nat. Rev. Immunol.* **2006**, *6* (7), 541−550.
(7) Clancy, D. M.; Sullivan, G. P.; Moran, H. B. T.; Henry, C. M.; Reeves, E. P.; McElvaney, N. G.; Lavelle, E. C.; Martin, S. J. Extracellular Neutrophil Proteases Are Efficient Regulators of IL-1, IL-33, and IL-36 Cytokine Activity but Poor Effectors of Microbial Killing. *Cell Rep.* **2018**, *22* (11), 2937−2950.
(8) Korkmaz, B.; Moreau, T.; Gauthier, F. Neutrophil Elastase, Proteinase 3 and Cathepsin G: Physicochemical Properties, Activity and Physiopathological Functions. *Biochimie* **2008**, *90* (2), 227−242.
(9) Korkmaz, B.; Horwitz, M.; Jenne, D.; Gauthier, F. Neutrophil Elastase, Proteinase 3, and Cathepsin G as Therapeutic Targets in Human Diseases. *Pharmacol. Rev.* **2010**, *62* (4), 726−759.
(10) Fritzsching, B.; Zhou-Suckow, Z.; Trojanek, J. B.; Schubert, S. C.; Schatterny, J.; Hirtz, S.; Agrawal, R.; Muley, T.; Kahn, N.; Sticht, C.; et al. Hypoxic Epithelial Necrosis Triggers Neutrophilic Inflammation via IL-1 Receptor Signaling in Cystic Fibrosis Lung Disease. *Am. J. Respir. Crit. Care Med.* **2015**, *191* (8), 902−913.
(11) Gehrig, S.; Mall, M. A.; Schultz, C. Spatially Resolved Monitoring of Neutrophil Elastase Activity with Ratiometric Fluorescent Reporters. *Angew. Chem., Int. Ed.* **2012**, *51* (25), 6258−6261.
(12) Dittrich, A. S.; Kühbandner, I.; Gehrig, S.; Rickert-Zacharias, V.; Twigg, M.; Wege, S.; Taggart, C. C.; Herth, F.; Schultz, C.; Mall, M. A. Elastase Activity on Sputum Neutrophils Correlates with Severity of Lung Disease in Cystic Fibrosis. *Eur. Respir. J.* **2018**, *51*, 1701910.
(13) Korkmaz, B.; Attucci, S.; Juliano, M. A.; Kalupov, T.; Jourdan, M. L.; Juliano, L.; Gauthier, F. Measuring Elastase, Proteinase 3 and Cathepsin G Activities at the Surface of Human Neutrophils with Fluorescence Resonance Energy Transfer Substrates. *Nat. Protoc.* **2008**, *3* (6), 991−1000.
(14) Guyot, N.; Wartelle, J.; Malleret, L.; Todorov, A. A.; Devouassoux, G.; Pacheco, Y.; Jenne, D. E.; Belaaouaj, A. Unopposed Cathepsin G, Neutrophil Elastase, and Proteinase 3 Cause Severe Lung Damage and Emphysema. *Am. J. Pathol.* **2014**, *184* (8), 2197−2210.
(15) Wilson, T. J.; Nannuru, K. C.; Futakuchi, M.; Singh, R. K. Cathepsin G-Mediated Enhanced TGF-β Signaling Promotes Angiogenesis via Upregulation of VEGF and MCP-1. *Cancer Lett.* **2010**, *288* (2), 162−169.
(16) Shafer, W. M.; Pohl, J.; Onunka, V. C.; Bangalore, N.; Travis, J. Human Lysosomal Cathepsin G and Granzyme B Share a Functionally Conserved Broad Spectrum Antibacterial Peptide. *J. Biol. Chem.* **1991**, *266* (1), 112−116.
(17) Pham, C. T. N. Neutrophil Serine Proteases Fine-Tune the Inflammatory Response. *Int. J. Biochem. Cell Biol.* **2008**, *40* (6), 1317−1333.
(18) Mu, J.; Liu, F.; Rajab, M. S.; Shi, M.; Li, S.; Goh, C.; Lu, L.; Xu, Q. H.; Liu, B.; Ng, L. G.; et al. A Small-Molecule Fret Reporter for the Real-Time Visualization of Cell-Surface Proteolytic Enzyme Functions. *Angew. Chem., Int. Ed.* **2014**, *53* (52), 14357−14362.
(19) Caughey, G. H. Mast Cell Tryptases and Chymases in Inflammation and Host Defense. *Immunol. Rev.* **2007**, *217* (1), 141−154.
(20) Yu, M.; Tsai, M.; Tam, S.; Jones, C.; Zehnder, J.; Galli, S. J. Mast Cells Can Promote the Development of Multiple Features of Chronic Asthma in Mice. *J. Clin. Invest.* **2006**, *116* (6), 1633−1641.
(21) Williams, C. M.; Galli, S. J. Mast Cells Can Amplify Airway Reactivity and Features of Chronic Inflammation in an Asthma Model in Mice. *J. Exp. Med.* **2000**, *192* (3), 455−462.
(22) Tanaka, T.; Minematsu, Y.; Reilly, C. F.; Travis, J.; Powers, J. C. Human Leukocyte Cathepsin G. Subsite Mapping with 4-Nitroanilides, Chemical Modification, and Effect of Possible Cofactors. *Biochemistry* **1985**, *24* (8), 2040−2047.
(23) Powers, J. C.; Tanaka, T.; Harper, J. W.; Minematsu, Y.; Barker, L.; Lincoln, D.; Crumley, K. V.; Fraki, J. E.; Schechter, N. M. Mammalian Chymotrypsin-like Enzymes. Comparative Reactivities of Rat Mast Cell Proteases, Human and Dog Skin Chymases, and Human Cathepsin G with Peptide 4-Nitroanilide Substrates and with Peptide Chloromethyl Ketone and Sulfonyl Fluoride Inhibitors. *Biochemistry* **1985**, *24* (8), 2048−2058.
(24) Raymond, W. W.; Su, S.; Makarova, A.; Wilson, T. M.; Carter, M. C.; Metcalfe, D. D.; Caughey, G. H. Alpha 2-Macroglobulin Capture Allows Detection of Mast Cell Chymase in Serum and Creates a Reservoir of Angiotensin II-Generating Activity. *J. Immunol.* **2009**, *182* (9), 5770−5777.
(25) Hunninghake, G. M.; Cho, M. H.; Tesfaigzi, Y.; Soto-Quiros, M. E.; Avila, L.; Lasky-Su, J.; Stidley, C.; Melén, E.; Söderhäll, C.; Hallberg, J.; et al. MMP12, Lung Function, and COPD in High-Risk Populations. *N. Engl. J. Med.* **2009**, *361* (27), 2599−2608.
(26) Brooks, C. R.; Van Dalen, C. J.; Hermans, I. F.; Douwes, J. Identifying Leukocyte Populations in Fresh and Cryopreserved Sputum Using Flow Cytometry. *Cytometry, Part B* **2013**, *84B* (2), 104−113.
(27) Taggart, C.; Coakley, R. J.; Greally, P.; Canny, G.; O'Neill, S. J.; McElvaney, N. G. Increased Elastase Release by CF Neutrophils Is Mediated by Tumor Necrosis Factor-α and Interleukin-8. *Am. J. Physiol. Cell. Mol. Physiol.* **2000**, *278* (1), L33−L41.
(28) Margaroli, C.; Garratt, L. W.; Horati, H.; Dittrich, A. S.; Rosenow, T.; Montgomery, S. T.; Frey, D. L.; Brown, M. R.; Schultz, C.; Guglani, L.; et al. Elastase Exocytosis by Airway Neutrophils Associates with Early Lung Damage in Cystic Fibrosis Children. *Am. J. Respir. Crit. Care Med.* **2018**, in press. DOI: 10.1164/rccm.201803-0442OC.
(29) Trojanek, J. B.; Cobos-Correa, A.; Diemer, S.; Kormann, M.; Schubert, S. C.; Zhou-Suckow, Z.; Agrawal, R.; Duerr, J.; Wagner, C. J.; Schatterny, J.; et al. Airway Mucus Obstruction Triggers Macrophage Activation and Matrix Metalloproteinase 12-Dependent Emphysema. *Am. J. Respir. Cell Mol. Biol.* **2014**, *51* (5), 709−720.
(30) Wichmann, O.; Wittbrodt, J.; Schultz, C. A Small-Molecule FRET Probe to Monitor Phospholipase A2 Activity in Cells and Organisms. *Angew. Chem., Int. Ed.* **2006**, *45* (3), 508−512.
(31) Scarabelli, S.; Tan, K. T.; Griss, R.; Hovius, R.; D'Alessandro, P. L.; Vorherr, T.; Johnsson, K. Evaluating Cellular Drug Uptake with Fluorescent Sensor Proteins. *ACS Sensors* **2017**, *2* (8), 1191−1197.
(32) Yu, Q.; Xue, L.; Hiblot, J.; Griss, R.; Fabritz, S.; Roux, C.; Binz, P.-A.; Haas, D.; Okun, J. G.; Johnsson, K. Semisynthetic Sensor Proteins Enable Metabolic Assays at the Point of Care. *Science (Washington, DC, U. S.)* **2018**, *361* (6407), 1122−1126.
(33) Yu, Y.-R. A.; Hotten, D. F.; Malakhau, Y.; Volker, E.; Ghio, A. J.; Noble, P. W.; Kraft, M.; Hollingsworth, J. W.; Gunn, M. D.; Tighe, R. M. Flow Cytometric Analysis of Myeloid Cells in Human Blood, Bronchoalveolar Lavage, and Lung Tissues. *Am. J. Respir. Cell Mol. Biol.* **2016**, *54* (1), 13−24.
(34) Stein, F.; Kress, M.; Reither, S.; Piljić, A.; Schultz, C. FluoQ - a Tool for Rapid Analysis of Multiparameter Fluorescence Imaging Data Applied to Oscillatory Events. *ACS Chem. Biol.* **2013**, *8* (9), 1862−1868.

DOI: 10.1021/acscentsci.8b00933
ACS Cent. Sci. 2019, 5, 539−548